Changes in the Heterogeneity of Cerebral Glucose Metabolism With Healthy Aging: Quantitative Assessment by Fractal Analysis

Jae Sung Lee
Dong Soo Lee
Kwang Suk Park
June-Key Chung
Myung Chul Lee

ABSTRACT

Background and Purpose. It has been shown that heterogeneity of cerebral glucose metabolism is increased in neuropsychiatric degenerative diseases. However, proper assessment of older patients requires knowledge about the effect of aging on heterogeneity. This study characterized the effects of aging on the heterogeneity of the distribution of cerebral glucose metabolism in healthy volunteers. *Methods*. Sixty-six healthy volunteers (age range, 19-75 years) underwent flurodeoxyglucose brain positron emission tomography (PET), and all the PET images were spatially normalized onto a previously segmented standard brain template to parcel the brain regions automatically. Fractal dimension was regarded as a quantitative measurement for the heterogeneity of cerebral glucose metabolism and obtained for 9 brain regions. Participants were subdivided into young/midlife and elderly groups, and the Student *t* test was applied to the comparison of fractal dimensions in those groups. Analysis of covariance was performed for each region to explore the effects of age, gender, age-by-gender interaction, and total counts in the brain on the observed metabolic heterogeneity. *Results*. Fractal dimensions were higher for elderly volunteers in most brain regions. Differences between the 2 groups in fractal dimension emerged within the whole gray matter, temporal lobe, striatum, and cingulate. No significant gender differences, age-by-gender interactions, or total counts were observed. Significant age effects were observed in the whole gray matter, frontal lobe, temporal lobe, striatum, and cingulate gyrus. *Conclusions*. Heterogeneity in the cerebral glucose metabolism of healthy volunteers increased with age, and individual variations of heterogeneity were higher in older volunteers. However, there was no significant difference between male and female volunteers of the same age. The effect of age on heterogeneity was not regionally uniform.

Key words: Heterogeneity, cerebral glucose metabolism, aging, positron emission tomography, normal volunteers.

Lee JS, Lee DS, Park KS, Chung J-K, Lee MC. Changes in the heterogeneity of cerebral glucose metabolism with healthy aging: quantitative assessment by fractal analysis. J Neuroimaging 2004;14:350-356. DOI:10.1177/1051228404268566

Received January 30, 2004, and in revised form June 4, 2004. Accepted for publication June 17, 2004.

From the Department of Nuclear Medicine (JSL, DSL, KSP, J-KC, MCL) and the Department of Biomedical Engineering (JSL, KSP), Seoul National University College of Medicine, Seoul, Korea.

Address correspondence to Dong Soo Lee, MD, PhD, Department of Nuclear Medicine, Seoul National University College of Medicine, 28 Yungun-Dong, Chongno-Gu, Seoul 110-799, Korea. E-mail: dsl@palza.snu.ac.kr.

Heterogeneity of the distribution of radiopharmaceuticals, or their underlying physiological parameters, has been assessed using various mathematical indices, including the coefficient of variation, entropy, and fractal dimension.[1-6] It has been shown that heterogeneity in cerebral blood flow (CBF) and glucose metabolism in neurodegenerative diseases, such as Alzheimer's disease, is altered compared to that of normal controls.[7-11] Nagao et al performed a series of investigations on the heterogeneity in the CBF in Alzheimer's disease using single-photon emission computed tomography (SPECT) and fractal analysis by the intensity thresholding method.[9,10] When they applied fractal analysis to the Tc-99m-HMPAO brain SPECT images of patients with probable Alzheimer's disease, the fractal dimension for the patients was significantly higher than in healthy control participants and correlated well with the degree of cognitive impairment, as assessed in neuropsychological tests.[10] Moreover, the patients with very early Alzheimer's disease, with mild cognitive impairment (grade 0.5 on a clinical dementia rate), could be segregated from normal controls by fractal dimension.[9]

However, proper assessment of elderly patients with neurodegenerative diseases, such as Alzheimer's disease, requires knowledge about the effects of aging. There have been many reports showing age- and/or gender-related

effects on the regional CBF,[12-14] glucose metabolism,[15-23] and several neuroreceptor systems.[24-26] Usually, those effects are regionally specific. Some regions are more vulnerable to these effects than are others. A linear model fits the data well for some regions, but nonlinear models are better in others. The regionally different pattern of such effects could alter the heterogeneity in distribution of radiotracers in the brain relative to age and/or gender.

The aim of this study was to characterize the effects of aging and gender on the heterogeneity of the distribution of cerebral glucose metabolism in healthy volunteers by fractal analysis[6,9,10] of F-18-flurodeoxyglucose (FDG) brain positron emission tomography (PET) images. This study examined whether there is an age-related alternation in the heterogeneity of the glucose metabolism in some brain regions and whether such trends can be observed in F-18-FDG brain PET imaging.

Methods

Participants

The study population consisted of 66 healthy volunteers with a mean age of 46.9 ± 17.5 years (age range, 19-75 years). There were 43 men and 23 women. The data were collected from ongoing PET research studies at Seoul National University Hospital. Exclusion criteria were current or prior history of any neurological or psychiatric disease or significant medical illnesses or past history of substance abuse. This study was carried out under guidelines for the use of human subjects established by the institutional review board at Seoul National University Hospital. After a complete description of the scope of the study was given to each participant, written informed consent was obtained. The volunteers were subdivided into 2 groups: a young/midlife group (age $<$ 55 years, n = 39, 28 men and 11 women) and an elderly group (age $>$ 55 years, n = 27, 15 men and 12 women).

F-18-FDG PET

PET studies were performed using an ECAT EXACT 47 scanner (Siemens-CTI, Knoxville, TN), which has an intrinsic resolution of 5.2 mm full width at half maximum and images 47 contiguous planes with a thickness of 3.4 mm simultaneously for a longitudinal field of view of 16.2 cm. Before F-18-FDG administration, transmission scanning was performed using 3 Ge-68 rod sources for attenuation correction. Static emission scans were started 30 minutes after the injection of 370 MBq (10 mCi) F-18-FDG and continued for 30 minutes. Transaxial images were reconstructed by means of a filtered back-projection algorithm, employing a Shepp-Logan filter with a cutoff frequency of 0.3 cycles/pixel, as 128 × 128 × 47 matrices with a size of 2.1 × 2.1 × 3.4 mm.

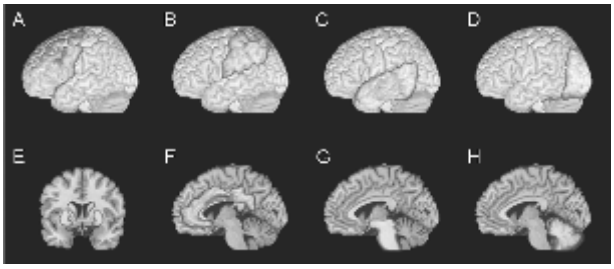

Fig 1. Volumes of interest superimposed on ICBM standard brain template. (A) Frontal lobe. (B) Parietal lobe. (C) Temporal lobe. (D) Occipital lobe. (E) Striatum. (F) Cingulate gyrus. (G) Brain stem. (H) Cerebellum.

Image Analysis

Using Statistical Parametric Mapping 99 (SPM99; Wellcome Department of Cognitive Neurology, London, UK) software,[27] all the images were spatially normalized onto International Consortium for Brain Mapping (ICBM) standard brain template, provided in SPM software, to remove the intersubject anatomic variability.[28,29] Affine transformation was performed to determine the 12 optimal parameters to register the brain on the template. Small differences between the transformed image and the template were removed by the nonlinear registration method, using the weighted sum of the predefined smooth basis functions used in discrete cosine transformation.[29]

The ICBM standard template was parceled into 9 volumes of interest (VOIs), as follows: whole gray matter, frontal lobe, parietal lobe, temporal lobe, occipital lobe, striatum, cingulate gyrus, brain stem, and cerebellum. Statistical Probabilistic Anatomical Map images of ICBM,[30-32] which are defined on ICBM standard template and consist of the probability from 0 to 1.0 belonging to specific regions, were classified into the above 9 regions and summed to compose the probabilistic map for these 9 regions (Fig 1). Voxels with a probability greater than .5 were finally included in each VOI.

To measure quantitatively the heterogeneity of the cerebral glucose metabolism, a fractal analysis, using the intensity thresholding method proposed by Nagao et al and applied to the analysis of heterogeneity in lung ventilation and brain perfusion SPECT images,[6,9,10] was applied to each VOI. Fractal dimension, a heterogeneity index, can be obtained by fitting the following equation, which relates a measure (M) to the scale (ε) of the ruler that measures M,

$$M(\varepsilon) = k \cdot \varepsilon^{-D}, \quad (1)$$

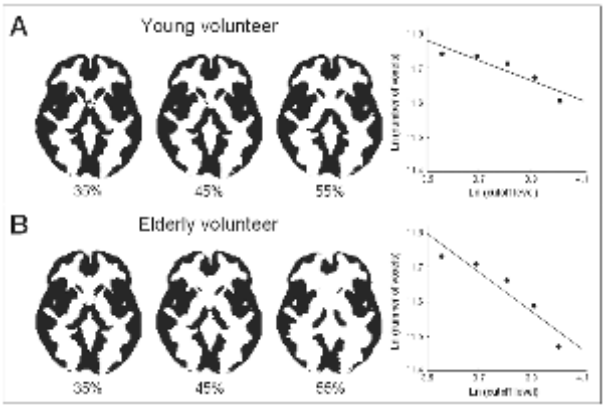

Fig 2. Segmented images obtained with each cutoff level (35%, 45%, and 55% of the mean of 1% highest voxel values) and plots between the natural logarithms of cutoff level and the number of voxels above that cutoff level to calculate the fractal dimension for whole gray matter. Images are spatially normalized to the standard template and masked using the probabilistic map of gray matter. (A) A 22-year-old man, whose fractal dimension for whole gray matter is 0.29. (B) A 60-year-old man, whose fractal dimension for whole gray matter is 0.56.

where k is the proportionality constant and D is a fractal dimension. The cutoff level to segment images was regarded as a scale ε, and the total number of voxels above each cutoff level was regarded as a measure M. For each VOI, total numbers of voxels above 5 cutoff levels (35%, 40%, 45%, 50%, and 55% of the mean of 1% highest voxel values in each VOI) were obtained, and the fractal dimension was calculated by relating the logarithms of cutoff level and number of voxels based on Equation 1 (Fig 2). We used 35% as a lower threshold because the background activity out of brain comes to be excluded from this threshold.

The total counts of the brain were also calculated to examine the effects of the total count, which is another potential confounder, on the fractal dimension.

Statistical Analysis

Participants were subdivided into 2 groups: a young/midlife group (age < 55 years) and an elderly group (age > 55 years). A 2-tailed Student t test was applied to the comparison of fractal dimension in young/midlife and elderly groups. The selection of age 55 is arbitrary, but this has been used as a threshold age to discriminate elderly participants from young/midlife in many cognitive and imaging researches. There is no definite criterion for this purpose.

To examine the effect of age, gender, age-by-gender interactions, and the total count on the heterogeneity of the cerebral glucose metabolism, independent analysis of covariance (ANCOVA) was performed for each VOI, with gender being the independent variable (grouping factor), age and the total count as the covariates, and the fractal dimension as the dependent variable. The associations between age and the fractal dimension were also tested using Pearson correlation analysis. The Bonferroni method was used for the multiple comparison correction, and a P value < .05 was considered significant. All the statistical analyses were carried out with SPSS 10.0 for Windows.

Table 1. Fractal Dimension ($\bar{x} \pm$ SD) in Young/Midlife Versus Elderly Volunteers

Region	Group	
	Young/Midlife	Elderly
Whole gray matter	0.224 ± 0.153	0.359 ± 0.186*
Frontal lobe	0.106 ± 0.046	0.145 ± 0.067
Parietal lobe	0.073 ± 0.033	0.087 ± 0.043
Temporal lobe	0.334 ± 0.160	0.464 ± 0.168*
Occipital lobe	0.216 ± 0.132	0.274 ± 0.180
Striatum	0.381 ± 0.157	0.573 ± 0.130†
Cingulate gyrus	0.071 ± 0.083	0.231 ± 0.133†
Brain stem	0.418 ± 0.279	0.501 ± 0.279
Cerebellum	0.187 ± 0.236	0.266 ± 0.334

*$P < .05$.
†$P < .00005$.

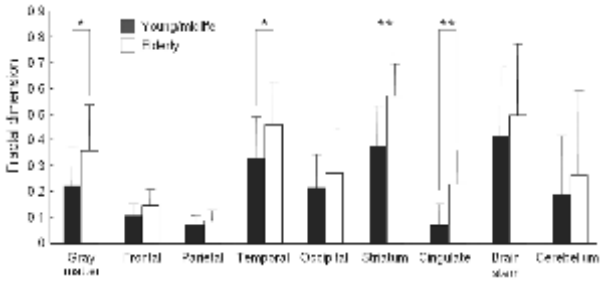

Fig 3. Bar graphs of mean fractal dimension in young/midlife versus elderly volunteers (*$P < .05$, **$P < .00005$, corrected for multiple comparisons).

Results

Fractal dimensions were higher for elderly volunteers relative to the young/midlife participants in all regions (Table 1; Fig 3). The difference between the 2 groups in fractal dimension was statically significant ($P < .05$, corrected for multiple comparisons) for the whole gray matter, temporal lobe, striatum, and cingulate gyrus (Table 1). Variance in the fractal dimension within each group was high compared to the differences between the 2 groups. For the whole gray matter, frontal lobe, parietal lobe, temporal lobe, striatum, and cingulate gyrus, the fraction of elderly volunteers who had a higher fractal dimension than the mean in young/midlife volunteers was 90%,

Table 2. Correlation Coefficient (r) Between Fractal Dimension and Age and Increase of Fractal Dimension per Decade of Age (ΔFD/Decade) for Each Volume of Interest

Region	r	ΔFD/Decade
Whole gray matter	0.402*	0.0408
Frontal lobe	0.358†	0.0118
Parietal lobe	0.251	0.0054
Temporal lobe	0.409*	0.0405
Occipital lobe	0.215	0.0189
Striatum	0.619‡	0.0611
Cingulate gyrus	0.661	0.0494
Brain stem	0.081	0.0128
Cerebellum	0.170	0.0271

*$P < .01$.
†$P < .05$.
‡$P < 5 \times 10^{-7}$.
§$P < 5 \times 10^{-8}$.

85%, 74%, 82%, 87%, and 95%, respectively. For those regions, the fraction of young/midlife volunteers who had a lower fractal dimension than the mean in elderly volunteers was 67%, 74%, 63%, 74%, 93%, and 85%, respectively.

No significant effects of gender differences, age-by-gender interactions, or total count were observed in any of the regions when ANCOVAs were employed. Significant age effects were observed in the whole gray matter ($F = 11.0$, $P < .05$, corrected for multiple comparisons), frontal lobe ($F = 9.70$, $P < .05$), temporal lobe ($F = 12.3$, $P < .01$), striatum ($F = 43.1$, $P < 5 \times 10^{-7}$), and cingulate gyrus ($F = 45.9$, $P < 1 \times 10^{-7}$).

In those regions, heterogeneity increased with age when analyzed by the Pearson correlation. Those correlations were moderate in the striatum and cingulate and weak in whole gray matter, frontal lobe, and temporal lobe. The correlation coefficient and increase of the fractal dimension per decade of age for each region are shown in Table 2.

Also noted is a trend that the variation in fractal dimension is higher in elderly volunteers than in young/midlife participants for most regions that show significant correlation with age except for the striatum (Table 1; Fig 4). Those differences in variance were not, however, statistically significant (F test).

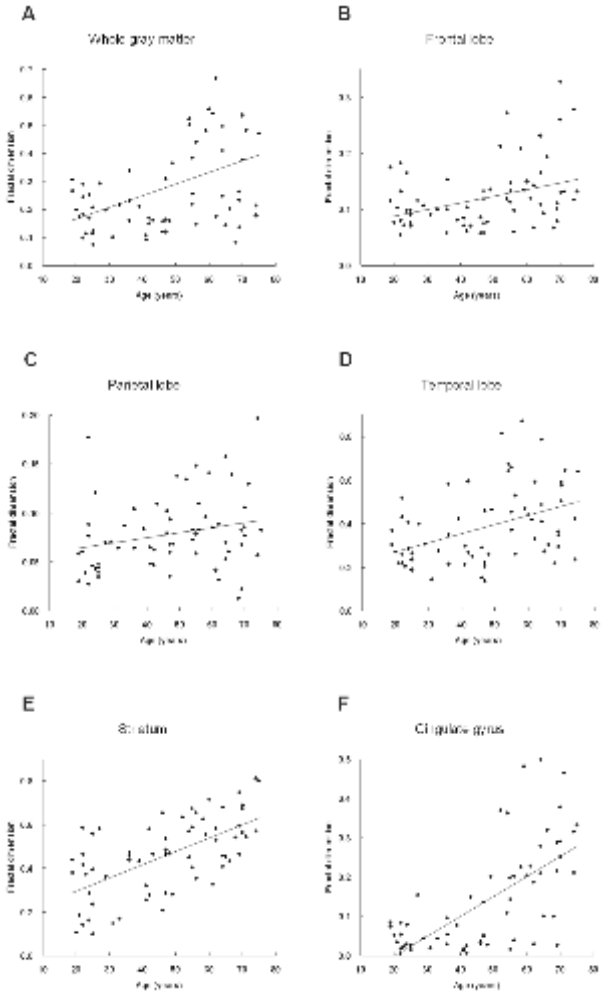

Fig 4. Scatterplot of fractal dimension versus age for the whole gray matter (A), frontal lobe (B), parietal lobe (C), temporal lobe (D), striatum (E), and cingulate gyrus (F).

Discussion

The findings of this study indicate that heterogeneity in cerebral glucose metabolism of healthy volunteers increased with age in the whole gray matter, frontal lobe, temporal lobe, striatum, and cingulate gyrus. Although such a trend was evident in the striatum and cingulate gyrus, the other regions showed weak correlations between fractal dimension and age. It should also be noted that some of the oldest participants had fractal dimensions that were less than many of the younger participants, and some very young participants had high fractal dimensions for some regions.

Age-related and regionally specific decreases in resting cerebral glucose metabolism and similar age-related declines in CBF and oxygen consumption have been reported in many articles in which modern, high-resolution PET scanners were used.[12-23] Consistently, the slope of the metabolic decline relative to the age and the degree of difference in metabolism between young and older people varied according to the regions examined. For example, in a recent study in which the effects of healthy aging on the regional cerebral glucose metabolism were assessed with SPM,[23] the bilateral and symmet-

rically distributed effects of age were most marked in the inferior and posterior lateral frontal, anterior cingulate, perisylvian temporoparietal and anterior temporal cortices, left caudate head, and anterior thalamus. However, the anterior dorsolateral prefrontal regions, posterior cingulate, precuneus, association occipital and inferior occipitotemporal cortices, as well as other areas, were relatively less affected, with no significant effects of age being identified in most of the occipital cortex.

Relative hypofrontality with increased age, and the lesser effects of age on the posterior brain shown in this example, are consistent findings of most previous studies and may provide pathologic substrate for the age-related deterioration in cognitive function and the slowing of information processing revealed in numerous behavioral experiments examining memory and other cognitive functions in elderly individuals.[33] The increase in heterogeneity of the cerebral glucose metabolism with an increase in age shown in this study could be explained, in part, by this anterior-posterior cortical metabolic gradient.[15,21,23]

A nonlinear decline of brain activity would augment the heterogeneity in the cerebral glucose metabolism. When Mozley et al investigated the aging effects on the CBF using HMPAO brain SPECT, they showed that a nonlinear "broken stick" regression model fit the data better than did a straight line.[14] In addition, breakpoint age, at which the 2 separate straight lines describing the CBF change with age intersect, was demonstrated and varied from 25 years and 40 years relative to the regions that fit the model.

Structural imaging studies have shown age-related loss of brain tissue to be more severe in the frontal lobes than elsewhere in the brain.[34] Therefore, a partial volume effect (PVE), due to cortical atrophy, would confound the results of investigation on the effects of healthy aging on the cerebral glucose metabolism. We did not correct for that PVE because structural MRI data for the participants were not available. Regionally different levels of cortical atrophy could alter the heterogeneity in the cerebral glucose metabolism measured by PET imaging, which has limited spatial resolution. However, the fractal analysis would be less sensitive to the PVE than an estimation of the mean pixel intensities in VOIs, which is the conventional quantification method. This is because the fractal dimension is obtained from the slope of the linear regression equation relating the natural logarithms of the cutoff level (ε) and the number of voxels (M). If the intensity level in a VOI is globally decreased (or increased) by the PVE, the number of voxels above each cutoff level will be scaled ($M \rightarrow k \times M$) due to the continuity of the intensity change in the boundary of the gray matter region. Scaling the number of voxels will alter the y intercept of the $\ln \varepsilon - \ln M$ plot, but the slope will be unaffected. However, it is possible that the fractal dimension is not totally free of the PVE because a local alteration of the intensity by the PVE within a VOI can modify the shape of the intensity histogram. Further investigations into the existence of an age-related effect on the heterogeneity in the cerebral glucose metabolism following a partial volume correction with structural MRI will be necessary.[35,36]

The effects of a possible error in the spatial normalization of the images should be considered because the spatial normalization and placement of the VOI is a crucial processing step in estimating the fractal dimension. Limitations in spatial normalization of a brain with age-related atrophy can lead to a poor fit of the VOIs with an associated increase or decrease in heterogeneity in some elderly participants. In the fractal analysis used in this study, the total numbers of voxels above 5 cutoff levels were obtained, and the fractal dimension was calculated by relating the cutoff level and the number of voxels. The lowest threshold, 35% of the mean of 1% highest voxel values in each VOI, was so high that most voxels above this threshold were included in the VOIs defined in this study using probabilistic maps. Therefore, there was low likelihood that errors in the spatial normalization and placement of the VOIs led to an incorrect estimation of the fractal dimension. However, a detailed analysis with the VOIs placed on a co-registered MRI will be needed to confirm this.

Heterogeneity in nuclear medicine image could be inversely related to the total counts due to the properties of Poisson statistics. However, no significant effect of the total count was observed in any of the regions. This might be because the fractal dimensions used in this study were estimated from the histogram of the counts. A histogram is less sensitive to the statistical noise associated with the total count because the fluctuations in the count are canceled out when the counts are combined into a histogram.

Two types of heterogeneity have been studied in the context of nuclear medicine research. Conceptually, the first (spatial heterogeneity) represents the heterogeneity of the spatial distribution of pixel counts. If pixels with similar counts are distributed randomly against a white background in an image, the image will appear heterogeneous; otherwise, it will appear homogenous. Fractal analysis using a box-counting technique[5,8] is a method used to evaluate such heterogeneity. The second type of heterogeneity (count heterogeneity) describes the heterogeneity of pixel counts in an image. If all pixels have the same value, the image will appear homogeneous; however, if the histogram of the image is a uniform distribution, it will appear heterogeneous. The standard devia-

tion, skew, or entropy of image histograms have been used to evaluate count heterogeneity. Nagao's method,[6,9,10] used in this study, is an example of such methods. Definitions and relationships of these types of heterogeneity can be found in the literature.[37]

Nagao's intensity thresholding method has been criticized.[38] Critics claim that the count heterogeneity does not represent the heterogeneity itself and that this type of heterogeneity would disappear by adjustment of the displaying window settings. However, in the interpretation of pathologic images, nuclear medicine physicians prefer count heterogeneity, which is caused by the regionally abnormal uptake of radiopharmaceuticals, and no one would ignore this pattern by intentionally widening the range of the color scale. Nagao's use of this method for the evaluation of CBF heterogeneity, shown in the brain perfusion SPECT images of the patients with Alzheimer's disease, is a good example.[9,10] Nagao showed how the count heterogeneity, frequently recognized in clinical situations, could be quantified using this method. Decline of the CBF in Alzheimer's disease displays a regionally dependent time course. In an early state of the disease, the CBF in the temporoparietal region declines first, and the regional CBF decrease spreads to frontal and other brain regions later. Nonetheless, the CBF is relatively preserved in primary sensory cortices. Therefore, the CBF distribution in Alzheimer's disease is more heterogeneous than in normal controls.

We agree with the criticism that the fractal nature of Nagao's equation is fractal only in its shape.[38] Counts that are distributed over a 3-dimensional space are in a single dimension in Nagao's framework and only mimic the complex fractal nature.

Conclusion

Heterogeneity in the cerebral glucose metabolism of healthy volunteers increased with age. However, no gender differences were identified, and the effect of age on heterogeneity was not regionally uniform.

This work was supported in part by the Ministry of Science and Technology of Korea and in part by the BK21 Human Life Sciences.

References

1. Thie JA. Degree of fractal behavior as a diagnostic aid in quantitative image analyses. *Mol Imaging Biol* 2003;5:227-231.
2. Yoshikawa T, Murase K, Oku N, et al. Statistical image analysis of cerebral blood flow in vascular dementia with small-vessel disease. *J Nucl Med* 2003;44:505-511.
3. Zhang X, Hirano H, Yamamoto K, et al. Technegas ventilation SPECT for evaluating silicosis in comparison with computed tomography. *Ann Nucl Med* 1996;10:165-170.
4. Barman SA, McCloud LL, Catravas JD, Ehrhart IC. Measurement of pulmonary blood flow by fractal analysis of flow heterogeneity in isolated canine lungs. *J Appl Physiol* 1996;81:2039-2045.
5. Kuikka JT, Tiihonen J, Karhu J, Bergstrom KA, Rasanen P. Fractal analysis of striatal dopamine re-uptake sites. *Eur J Nucl Med* 1997;24:1085-1090.
6. Nagao M, Murase K, Yasuhara Y, Ikezoe J. Quantitative analysis of pulmonary emphysema: three-dimensional fractal analysis of single-photon emission computed tomography images obtained with a carbon particle radioaerosol. *Am J Roentgenol* 1998;171:1657-1663.
7. Tiihonen J, Kuikka J, Rasanen P, et al. Cerebral benzodiazepine receptor binding and distribution in generalized anxiety disorder: a fractal analysis. *Mol Psychiatry* 1997;2:463-471.
8. Kuikka JT, Repo E, Bergstrom KA, Tupala E, Tiihonen J. Specific binding and laterality of human extrastriatal dopamine D2/D3 receptors in late onset type 1 alcoholic patients. *Neurosci Lett* 2000;292:57-59.
9. Nagao M, Murase K, Kikuchi T, et al. Three-dimensional fractal analysis of cerebral blood flow distribution in very early Alzheimer's disease [abstract]. *J Nucl Med* 2000;41(suppl):227P.
10. Nagao M, Murase K, Kikuchi T, et al. Fractal analysis of cerebral blood flow distribution in Alzheimer's disease. *J Nucl Med* 2001;42:1446-1450.
11. Cho S, Lee JS, Lee DS, Soh KS, Chung J-K, Lee MC. Heterogeneity of cerebral glucose metabolism in Alzheimer's disease [abstract]. *J Nucl Med* 2000;41(suppl):227P.
12. Martin AJ, Friston KJ, Colebatch JG, Frackowiak RS. Decreases in regional cerebral blood flow with normal aging. *J Cereb Blood Flow Metab* 1991;11:684-689.
13. Schultz SK, O'Leary DS, Boles Ponto LL, Watkins GL, Hichwa RD, Andreasen NC. Age-related changes in regional cerebral blood flow among young to mid-life adults. *Neuroreport* 1999;10:2493-2496.
14. Mozley PD, Sadek AM, Alavi A, et al. Effects of aging on the cerebral distribution of technetium-99m hexamethylpropylene amine oxime in healthy humans. *Eur J Nucl Med* 1997;24:754-761.
15. Willis MW, Ketter TA, Kimbrell TA, et al. Age, sex and laterality effects on cerebral glucose metabolism in healthy adults. *Psychiatry Res* 2002;114:23-37.
16. Loessner A, Alavi A, Lewandrowski KU, Mozley D, Souder E, Gur RE. Regional cerebral function determined by FDG-PET in healthy volunteers: normal patterns and changes with age. *J Nucl Med* 1995;36:1141-1149.
17. Kawachi T, Ishii K, Sakamoto S, Matsui M, Mori T, Sasaki M. Gender differences in cerebral glucose metabolism: a PET study. *J Neurol Sci* 2002;199:79-83.
18. Gur RC, Mozley LH, Mozley PD, et al. Sex differences in regional cerebral glucose metabolism during a resting state. *Science* 1995;267:528-531.
19. Murphy DG, DeCarli C, McIntosh AR, et al. Sex differences in human brain morphometry and metabolism: an in vivo quantitative magnetic resonance imaging and positron emission tomography study on the effect of aging. *Arch Gen Psychiatry* 1996;53:585-594.

20. Volkow ND, Wang GJ, Fowler JS, et al. Gender differences in cerebellar metabolism: test-retest reproducibility. *Am J Psychiatry* 1997;154:119-121.
21. Moeller JR, Ishikawa T, Dhawan V, et al. The metabolic topography of normal aging. *J Cereb Blood Flow Metab* 1996; 16:385-398.
22. Blesa R, Mohr E, Miletich R, et al. Changes in cerebral glucose metabolism with normal aging. *Eur J Neurol* 1997;4:8-14.
23. Petit-Taboue MC, Landeau B, Desson JF, Desgranges B, Baron JC. Effects of healthy aging on the regional cerebral metabolic rate of glucose assessed with statistical parametric mapping. *Neuroimage* 1998;7:176-184.
24. Ichise M, Ballinger JR, Tanaka F, et al. Age-related changes in D2 receptor binding with iodine-123-iodobenzofuran SPECT. *J Nucl Med* 1998;39:1511-1518.
25. Lavalaye J, Booij J, Reneman L, Habraken JB, van Royen EA. Effect of age and gender on dopamine transporter imaging with [123I]FP-CIT SPECT in healthy volunteers. *Eur J Nucl Med* 2000;27:867-869.
26. Pirker W, Asenbaum S, Hauk M, et al. Imaging serotonin and dopamine transporters with 123I-beta-CIT SPECT: binding kinetics and effects of normal aging. *J Nucl Med* 2000;41:36-44.
27. Friston KJ, Holmes AP, Worsley KJ, Poline J-P, Frith CD, Frackowiak RSJ. Statistical parametric maps in functional imaging: a general linear approach. *Hum Brain Mapp* 1995;2:189-210.
28. Friston KJ, Ashburner J, Frith CD, Poline J-B, Heather JD, Frackowiak RSJ. Spatial registration and normalization of images. *Hum Brain Mapp* 1995;2:165-189.
29. Ashburner J, Friston KJ. Nonlinear spatial normalization using basis functions. *Hum Brain Mapp* 1999;7:254-266.
30. Mazziotta JC, Toga AW, Evans A, Fox P, Lancaster J. A probabilistic atlas of the human brain: theory and rationale for its development. The International Consortium for Brain Mapping (ICBM). *Neuroimage* 1995;2:89-101.
31. Evans AC, Collins DL, Holmes CJ. Computational approaches to quantifying human neuroanatomical variability. In: Toga AW, Mazziotta JC, eds. *Brain Mapping: The Methods.* San Diego, CA: Academic Press; 1996:343-361.
32. Kang KW, Lee DS, Cho JH, et al. Quantification of F-18 FDG PET images in temporal lobe epilepsy patients using probabilistic brain atlas. *Neuroimage* 2001;14:1-6.
33. Grady CL. Functional brain imaging and age-related changes in cognition. *Biol Psychol* 2000;54:259-281.
34. Coffey CE, Wilkinson WE, Parashos IA, et al. Quantitative cerebral anatomy of the aging human brain: a cross-sectional study using magnetic resonance imaging. *Neurology* 1992;42:527-536.
35. Meltzer CC, Leal JP, Mayberg HS, Wagner HN Jr, Frost JJ. Correction of PET data for partial volume effects in human cerebral cortex by MR imaging. *J Comput Assist Tomogr* 1990;14:561-570.
36. Mueller-Gaertner HW, Links JM, Prince JL, et al. Measurement of radiotracer concentration in brain gray matter using positron emission tomography: MRI-based correction for partial volume effects. *J Cereb Blood Flow Metab* 1992;12:571-583.
37. Pitard FF. *Pierre Gy's Sampling Theory and Sampling Practice: Heterogeneity, Sampling Correctness, and Statistical Process Control.* 2nd ed. Boca Raton, FL: CRC Press; 1993.
38. Chung HW, Huang YH. Fractal analysis of nuclear medicine images for the diagnosis of pulmonary emphysema: interpretations, implications, and limitations. *Am J Roentgenol* 2000;174:1055-1059.